Vision Res. Vol. 14, pp. 1409-1420. Pergamon Press 1974. Printed in Great Britain.

SPATIAL FREQUENCY CHANNELS IN HUMAN VISION AS ASYMMETRIC (EDGE) MECHANISMS

C. F. STROMEYER **III** and S. KLEIN[1]
Department of Psychology, Stanford University, Stanford, California 94305, U.S.A.

(Received 12 *September* 1973)

Abstract—The detectability of a 9·0 c/deg sinusoidal grating was measured against various backgrounds: A blank field, a 3·0 c/deg grating and a 1·8 c/deg grating. Detection of the 9·0 c/deg grating was facilitated by suprathreshold 3·0 c/deg grating backgrounds (3·0 and 9·0 c/deg are first and third harmonics), but was not facilitated by 1·8 c/deg grating backgrounds (first and fifth harmonics). The results can be explained by channels whose sensitivity to spatial frequencies has an octave bandwidth. The channels respond to both gratings which are separated by a 1:3 ratio, but they do not respond significantly to both gratings which are separated by a 1:5 ratio. The results suggest that the channels used in the *detection of gratings* have a bandwidth similar to the channels revealed by adaptation and masking studies. Analysis of phase sensitivity suggests that the mechanisms have an asymmetric receptive field (edge mechanisms).

INTRODUCTION

The existence of mechanisms (channels) within the human visual system which are selectively sensitive to different limited ranges of spatial frequencies has been proposed on the basis of psychophysical studies. These studies typically employ patterns of stripes called sinusoidal gratings, in which the luminance along a vertical line is constant and the luminance along a horizontal line varies sinusoidally. Spatial frequency is simply the number of cycles per degree of visual angle.

At present there is considerable controversy over the degree of tuning of these postulated mechanisms. Evidence for *medium* bandwidth channels with a bandwidth of approximately an octave is provided by adaptation and masking studies (Pantle and Sekuler, 1968; Blakemore and Campbell, 1969; Graham, 1972; Stromeyer and Julesz, 1972). (An octave change in spatial frequency doubles or halves the frequency.) Blakemore and Campbell found that after prolonged observation of a high-contrast sinusoidal grating, gratings of similar spatial frequency were harder to detect—more contrast was needed to see them at threshold. This threshold elevation effect is strongest for test gratings which match the adapting frequency, and the effect falls to half strength at about 0·5 octave either side of the adapting frequency—hence, a bandwidth of 1 octave. Weak effects were observed with test gratings out to about 2 octaves below and 1·25 octaves above the adaptation frequency. Stromeyer and Julesz (1972) observed a similar spatial frequency dependence between the visibility of a vertical sinusoidal test grating and a *superposed* field of vertical noise stripes of specific bandwidth. That is, the noise acted like an adapting grating in raising the threshold contrast of the test grating. The apparent spatial frequency shift (Blakemore and Sutton, 1969) and contour contingent color aftereffects, the McCollough effect (Stromeyer, Lange and Ganz, 1973) also provide evidence for the existence of medium bandwidth channels.

Evidence for narrow bandwidth channels with a 1/3 octave bandwidth comes from a facilitation study by Sachs, Nachmias and Robson (1971; see also Lange, Sigel and Stecher, 1973; Kulikowski and King-Smith, 1973) who examined the visibility of a linear superposition of two *subthreshold* gratings. Detection of the composite grating was measured as a function of the frequency separation between the two sinusoids. Only gratings with similar spatial frequencies facilitated each other: Gratings separated by one octave did not facilitate the detection of each other—at least for gratings above 2·8 c/deg. The tuning curve for a channel centered at 14 c/deg was indeed sharp; sensitivity was reduced to about 1/3 maximum value only 20 per cent either side of the peak frequency—hence, a bandwidth of about 1/3 octave.

Evidence for broadband channels with a two octave bandwidth comes from studies on subthreshold facilitation which show that gratings with a very wide range of spatial frequencies can facilitate detection of edges (Shapley and Tolhurst, 1973; Kulikowski and King-Smith, 1973).

The different tuning characteristics may indicate the existence of different types of mechanisms that selectively fire to gratings, lines, edges and other stimuli. An alternative interpretation is that different weightings or arrangements of similar types of elementary mechanisms, are used in detecting different stimuli. Thus several medium-band mechanisms, all at the same position but with different peak frequencies may be used for detecting edges and bars.

[1] Present address: Joint Science Department, Claremont Colleges, Claremont, CA 91711, U.S.A. Send reprint requests to this address.

Likewise, several medium-band mechanisms of similar peak spatial frequencies but different spatial positions may be used to detect a grating. In the experiments that show narrow-band mechanisms, gratings of similar frequencies are superimposed. The contrast of the two gratings will add where the gratings are in phase, but at other regions the contrast will subtract where the gratings are out of phase—the pattern thus contains contrast beats. Several medium-band mechanisms at different spatial positions may participate in detection of the pattern, and detection may be based on some *average* contrast value rather than on simply the peak contrast. This would produce the illusion of a narrow-band channel. Evidence against narrow-band channels, within the range of 3-6 c/deg, is presented by Stromeyer and Klein (1975) who found that a frequency modulated grating is about as detectable as a regular sinusoidal grating. The modulated grating is *constant* in contrast across the whole grating and thus contains no contrast beats. The spectral components of the grating are widely spaced and thus narrow-band channels cannot respond well to more than one component. The results demonstrate that gratings are not detected by narrow-band channels, within the range of 3-6 c/deg, but may be detected by medium-band channels.

The present experiment is similar to that of Sachs *et al* except that one of the gratings is suprathreshold. Our results suggest that there exist separate spatial frequency channels with medium bandwidth characteristics—compatible with the adaptation and masking studies. The detectability of a test grating is measured using different backgrounds. Backgrounds consist of either a blank field or a second low-contrast grating which *may be clearly visible.* The detectability of the test grating was found to be facilitated by the grating background, provided that the spatial frequency separation between the test and background gratings was not too great. The results suggest that the mechanism used to detect the test grating can also respond to the background grating. Analysis of the results in the Discussion further suggests that these mechanisms have asymmetric receptive fields (edge mechanisms).

METHODS

Apparatus

Vertical sinusoidal gratings were generated on the face of a CRT following the methods of Campbell and Green (1965). One sine-wave generator triggered both the X-axis sweep and a second sine-wave generator (Wavetek Model 112). Both sine-wave generators were used to modulate the Z-axis of the oscilloscope. In this manner, vertical gratings consisting of either one sinusoidal grating or two phase-locked superimposed sinusoidal gratings could be displayed on the oscilloscope.

The display was a circular field 4° dia with a black surrounding mask. Viewing distance was 122 cm. Fine diagonal cross hairs were placed on the field to aid focussing. The mean spatial luminance of the scope was maintained at 5·0 cd/m^2 at all times. The CRT had a white phosphor, P-4.

The spatial frequency of the gratings was set with a digital frequency meter. The grating modulation voltage was set with a VTVM. A second oscilloscope was used to ascertain that the relative phase or the frequency of the two sinusoidal gratings did not drift. Contrast of the gratings is conventionally defined

$$c = \frac{L_{max} - L_{min}}{L_{max} + L_{min}}.$$

Sinusoidal gratings of 0·8 contrast, with little harmonic distortion, were readily obtained. The contrast of the gratings used throughout the experiments, however, was usually confined below about 0·1.

Procedure

The subject's task was simply to detect the presence of a 9·0 c/deg sinusoidal test grating which was displayed for a short duration. This test grating was displayed on different backgrounds as illustrated in Fig. 1. The backgrounds were:

(1) A blank field.

(2) A 3·0 c/deg grating shown at various contrast levels. The gratings were usually in peaks-subtract phase, i.e. the peak of the 3·0 c/deg grating coincided with the trough of the 9·0 c/deg grating. This will also be called square-wave phase, since the two components have the same phase relationship as the first and third harmonic of a square-wave. In a few instances the gratings were in peaks-add phase, or triangle-wave phase. These gratings have a 1:3 frequency ratio—hence first and third harmonics.

(3) A 1·8 c/deg grating shown at various contrast levels. The 9·0 c/deg grating was always in square-wave phase, where, in this case, peaks-add. These gratings

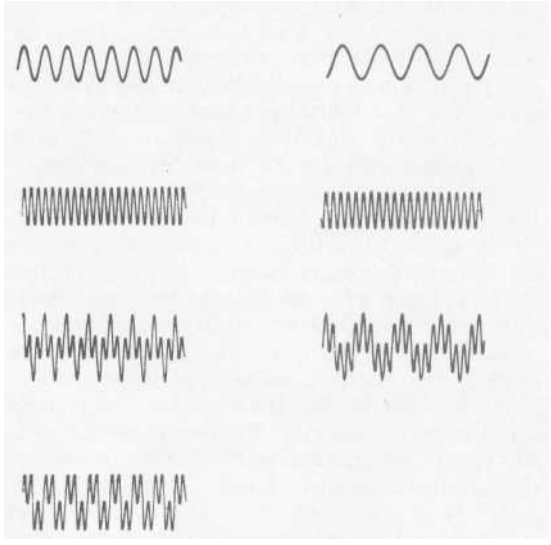

Fig. 1. Profiles of stimuli. Left column going downward: 3·0 c/deg background grating, 9·0 c/deg test grating, background and test summed in peaks-add phase, background and test summed in peaks-subtract phase. Right column going downward: 1·8 c/deg background grating, 9·0 c/deg test grating, background and test grating summed in peaks-add phase. As shown here, the amplitudes of the simple gratings are equal, but in the experiments, the amplitude of the test pattern was typically much smaller than the amplitude of the background grating.

have a 1:5 frequency ratio—hence first and fifth harmonics.

(4) A 9·0 c/deg grating at various contrast levels. The 9·0 c/deg test grating was presented in phase with this background grating.

The stimuli were presented in a continuously repeating sequence:

(1) 4-sec, blank field.

(2) 4-sec, tone plus test pattern b*ackground*. During this period, *S* pressed a button which, on about 50 per cent of the occasions, presented the 9·0 c/deg test grating for approximately 750 msec. The onset and offset of the test grating produced *no* visible electrical noise on the CRT.

For a given run, both the contrast of the 9·0 c/deg test grating and the contrast of the test pattern background were kept constant. A run consisted of 50 trials. On each trial *S* pressed the button to present the test pattern; the pattern appeared on about 50 per cent of the trials (a signal), as determined by a random number table—on the other 50 per cent of the trials, no test pattern appeared (a blank). The subject's task was simply to report on the presence of the *test pattern* using a confidence rating scale. The subject rated each trial with a whole number, 1-5, where 1 means definitely a blank and 5 means definitely a test grating (Egan, Schulman and Greenberg, 1959). After each response, the subject was informed whether the trial had been a blank or a signal.

The detectability d' is given by the horizontal intercept of the ROC curve plotted on double-axis z score (standard score) paper. To make this clear, imagine that the subject has a 50 per cent chance of correctly identifying a signal (hit rate), then the z score of the false alarm rate is $-d'$ or equivalently, the correct rejection of blanks is d'. For example, a 50 per cent hit rate and 84 per cent correct rejection of blanks, gives $d' = 1$. In order to extrapolate from the data point to this horizontal intercept, the slope of the ROC curve a found by Nachmias and Kocher (1970) was used.

$$d' = z_s/\alpha - z_n$$

where $1/7 = 1 + 0{\cdot}25\,d'$. Thus $d' = (z_s - z_n)/(1\text{-}0{\cdot}25z_s)$.

Other choices for the ROC slope (such as a = 1) would not alter the conclusions. The choice of slope used here is also supported by studies on the detection of gratings (Klein, Stromeyer and Dawson, in preparation).

The standard error of each data point can be obtained by using the assumptions of signal detection theory. The calculations are given in Klein, Stromeyer and Ganz (1974). The expected standard error of d' in the present paper is between 0·4 and 0·5 when d' is less than 2·5. The error is somewhat greater for higher values of d'. These values of the standard error are in agreement with the scatter of the data points.

At the beginning of each session, the subject had a few practice trials until he was satisfied that he was ready to start the run. The scope was viewed with the left eye, which was carefully refracted, and the subject's head was held with a brow and chin rest.

Various results were repeated several months after initial measurements, with no noticeable changes in the results. All data are shown in the Results.

RESULTS

The detectability d' of the 9·0 c/deg grating presented on the blank background is shown in Fig. 2 for subject SK. Contrast of the grating is represented on the abscissa. A given symbol is used throughout for data collected on a given day. Detectability increases rapidly over a contrast range of less than two-fold. For subsequent parts of the experiment, various contrast levels within this narrow range were chosen to see whether the detectability of the 9·0 c/deg could be facilitated by backgrounds consisting of other gratings. All curves fitted to the data are described in the Discussion.

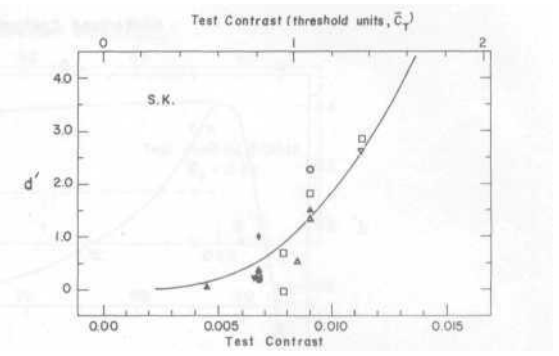

Fig. 2. The detectability d' of the 9·0 c/deg sinusoidal test grating on a blank background as a function of grating contrast. A given symbol is used throughout the experiments for data collected on a given day. The solid line is the transducer function which is used throughout this study. The form of the transducer function is given in the Discussion. The upper abscissa shows contrast in units of the threshold contrast. Threshold contrast is defined as the point where $d' = 1$. Subject: SK.

Figure 3 shows for subject SK the detectability of the 9·0 c/deg test grating, at a contrast level of 0·0068, superposed in phase on a background grating of the identical spatial frequency. The contrast of the *background* grating is represented on the abscissa. For zero contrast of the background, d' is approximately 0·5; d', however, increases rapidly as the contrast of the background grating is increased up to about 0·015 contrast, and, thereafter, with further increases in the contrast of the background grating, d' decreases. These results demonstrate that it is easier to detect a small increment in the contrast of a low-contrast 9·0 c/deg grating than it is to detect the same contrast increment against a blank background. This clearly suggests that the mechanism that responds to the background grating also responds to the test grating—the contrast increment. [A similar facilitation effect was noted by Camphell and **Kulikowski** (1966) and by Nachmias and Sansbury (1974).] Now, we ask whether this facilitation effect will occur when the spatial frequency of the background grating is made quite different from the frequency of the test grating: Facilitation would imply that the mechanism used in detecting the test grating is also affected by the background grating; conversely, no facilitation would imply that no single mechanism is affected by both the test grating and background grating.

Figures 4 and 5 show the detectability of the 9·0 c/deg grating superposed on background gratings of 3·0 c/deg. Each figure is for a different subject, SK and

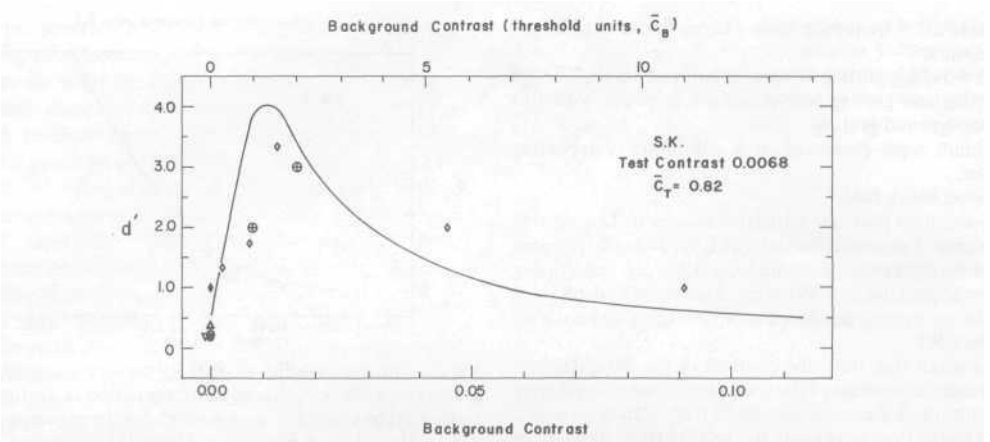

Fig. 3. Detectability of the 9·0 c/deg test grating added in phase on a 9·0 c/deg background grating. The contrast of the test grating was 0·0068 (or $\bar{c}_T = 0{\cdot}82$, in units of threshold contrast). The abscissa shows the background contrast. The solid line is the prediction from the transducer function as described in the Discussion. Subject: SK.

CFS. Each panel is for a different contrast level of the 9·0 c/deg *test* grating. The contrast of the 3·0 c/deg background grating is represented on the abscissa. At the far left on the abscissa, background contrast is zero. As background contrast increases, *d'* also increases. The test grating, in most instances, is added on the background grating in peaks-subtract phase (square-wave phase). Symbols surrounded by small dotted cages, however, represent instances in which the test grating was added in peaks-add phase (triangle-wave phase). For a constant background contrast, the detectability of the test grating is always somewhat higher when added to the background in peaks-subtract phase than when added in peaks-add phase. (The implications of this phase sensitivity are considered in the Discussion.)

These results, which show that a 3·0 c/deg background grating can facilitate the detection of the 9·0 c/deg test grating, suggest that a single mechanism responds to both components. Does this mechanism have a very wide bandwidth; that is, will a larger frequency separation between test and background gratings still yield a facilitation effect? Figure 6 shows the detectability of the 9·0 c/deg test grating on background gratings of 1·8 c/deg (frequency ratio 1:5). The contrast of the background grating is again represented on the abscissa. Top panel is for subject SK; bottom panel, for CFS. Note that the contrast of the test pattern is different for each subject. Little facilitation is observed.

Similar results were obtained in some limited experiments when the frequencies of the background and test gratings were all trebled to 5·4, 9·0 and 27·0 c/deg.

It was also observed that the converse type of experiment did not appear to yield facilitation: A fine background grating of 9·0 c/deg did not appear to facilitate the detection of a coarse 3·0 c/deg grating. This task, however, seemed subjectively very different. The test grating was seen through or behind the fine background grating, and the test grating did not appear to change the shape of the background grating. In the other task in which the 9·0 c/deg grating was added to the 3·0 c/deg background grating, the subject attempted to perceive the change in shape of single bars of the background grating caused by brief addition of the test grating—for example, the edge of the bars might appear to suddenly sharpen.

DISCUSSION

Our basic result is that the detectability of a 9·0 c/deg grating was facilitated when the pattern was added in peaks-subtract or peaks-add phase on a *clearly visible* 3·0 c/deg grating. However, when the frequency separation between the test and background grating was increased from 1:3 to 1:5, detection of the test pattern was no longer facilitated by the background grating.

These results contrast with those of Campbell and Robson (1968) who observed that a sinusoidal and square-wave grating are just detectably different when the patterns are of sufficient amplitude for the third harmonic of the square-wave to reach its own threshold—the threshold determined by measuring the threshold of the third harmonic presented *alone*. The present results show that the visibility of a third harmonic (9·0 c/deg) test grating was often enhanced when added onto a clearly visible first harmonic (3·0 c/deg) background grating. A very weak test pattern could change the *appearance* of the background grating. For example, when the 9·0 c/deg test pattern was set to threshold or even subthreshold contrast by the method of adjustment, and then momentarily added to the 3·0 c/deg background grating in peaks-subtract phase, the background grating appeared decidedly more truncated or squarish.

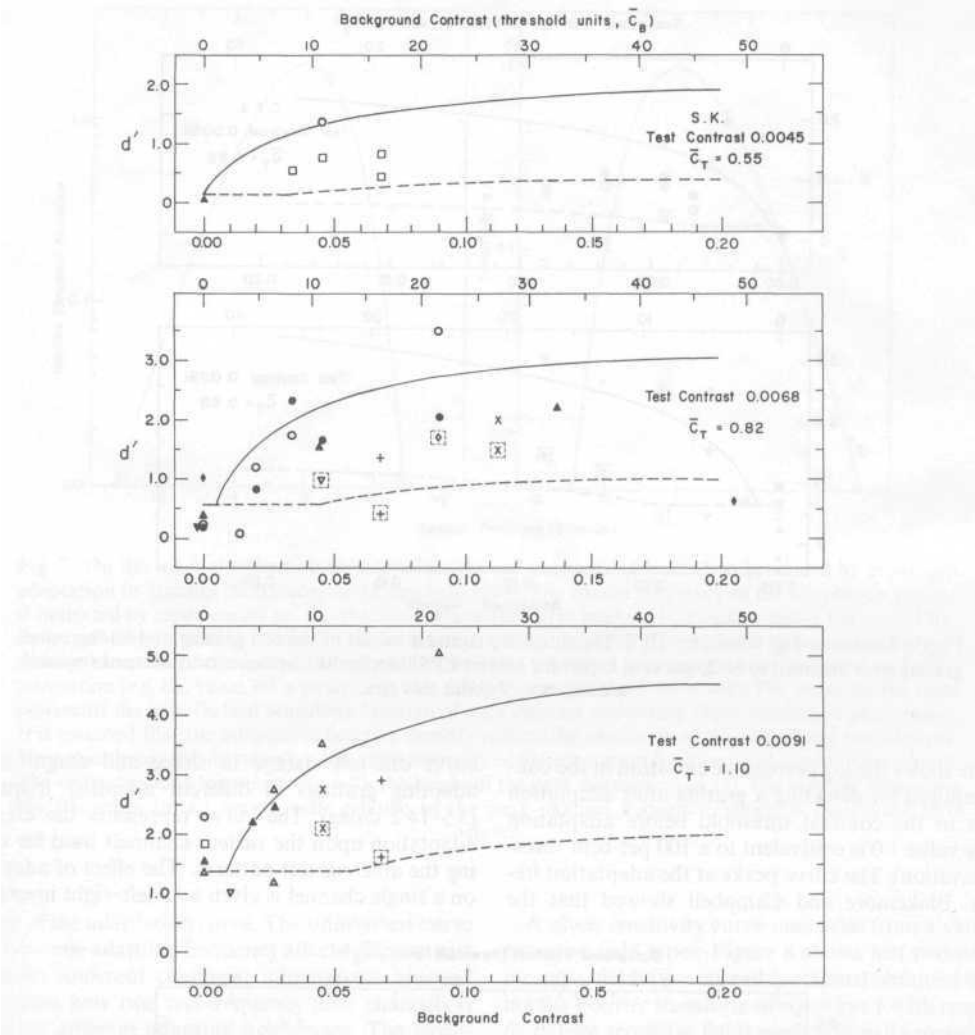

Fig. 4. Detectability of the 9·0 c/deg test grating added to a 3·0 c/deg background grating. Data in dotted cages are for test grating added in peaks-add phase; all other data are for test grating in peaks-subtract phase. Each panel is for a different contrast level of the test grating. Background contrast is shown on the lower abscissa; on the upper abscissa background contrast is given in units of threshold contrast, $\bar{c}_B$. The threshold contrast of the background was assumed to be one half the threshold contrast of the test pattern, because the photopic contrast sensitivity function shows that the threshold contrast for a grating of 3·0 c/deg is approximately one half of the value of the 9·0 c/deg grating. The solid curve is the prediction for the matched phase-selective mechanism; dashed line, for the non-matched mechanism (see Discussion). Subject: SK.

The results are compatible with the assumption that there are medium bandwidth channels which are broad enough to respond to two grating components separated by a 1:3 frequency ratio, but which are not so broad as to respond vigorously to two components separated by a 1:5 frequency ratio. The channels found in adaptation (Blakemore and Campbell) and masking studies (Stromeyer and Julesz) have a similar bandwidth. Channels whose peak frequencies lie between the frequency of the background and test grating may respond significantly to both components. The background grating may bring the response of the channels up near "threshold", thus making the channels more sensitive to the test pattern. A quantitative model will be developed to explain the results on the basis of medium-band channels.

Figure 7, left half, shows the curve that Blakemore and Campbell used to fit their adaptation data. The subject adapts to one frequency and is tested with gratings of various frequencies—the abscissa represents the frequency of the test patterns on an octave scale relative to the adaptation frequency, at 0 octaves. The

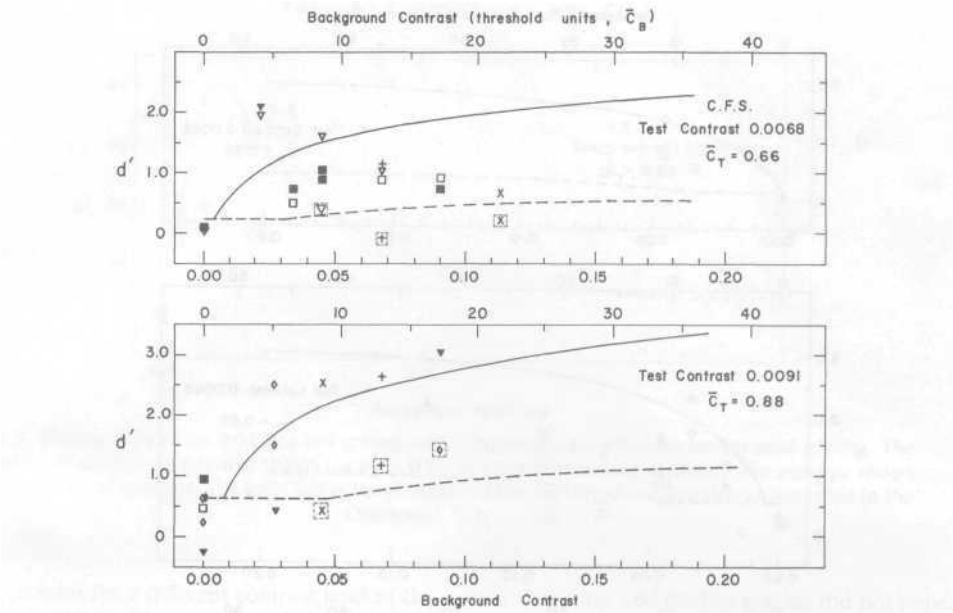

Fig. 5. Similar to Fig. 4, subject: CFS. The threshold contrast values of the test grating and background grating were assumed to be 25 per cent higher for subject CFS than for SK, because measurement revealed a difference of about this size.

ordinate shows the log percentage elevation in the contrast required for detecting a grating after adaptation relative to the contrast threshold before adaptation (e.g. the value 1·0 is equivalent to a 100 per cent threshold elevation). The curve peaks at the adaptation frequency. Blakemore and Campbell showed that the curve did not change in shape and magnitude for adapting gratings of different adapting frequencies (3·5-14·2 c/deg). The curve represents the effects of adaptation upon the *various* channels used for detecting the *different* test patterns. The effect of adaptation on a single channel is given by a left-right inversion of

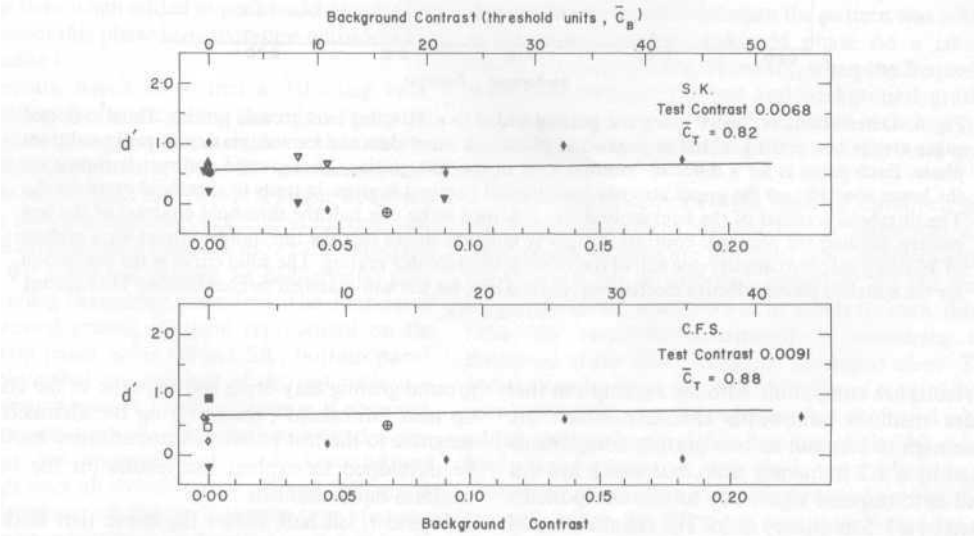

Fig. 6. Detectability of the 9·0 c/deg test grating added in peaks-add phase on a 1·8 c/deg background grating. The contrast of the test grating was 0·0068 for subject SK and 0·0091 for CFS. The abscissa shows the background contrast. The threshold contrast of the background is assumed to have the same value as the 3·0 c/deg background (Figs. 4 and 5). The solid curve is the prediction for the matched phase-selective mechanism.

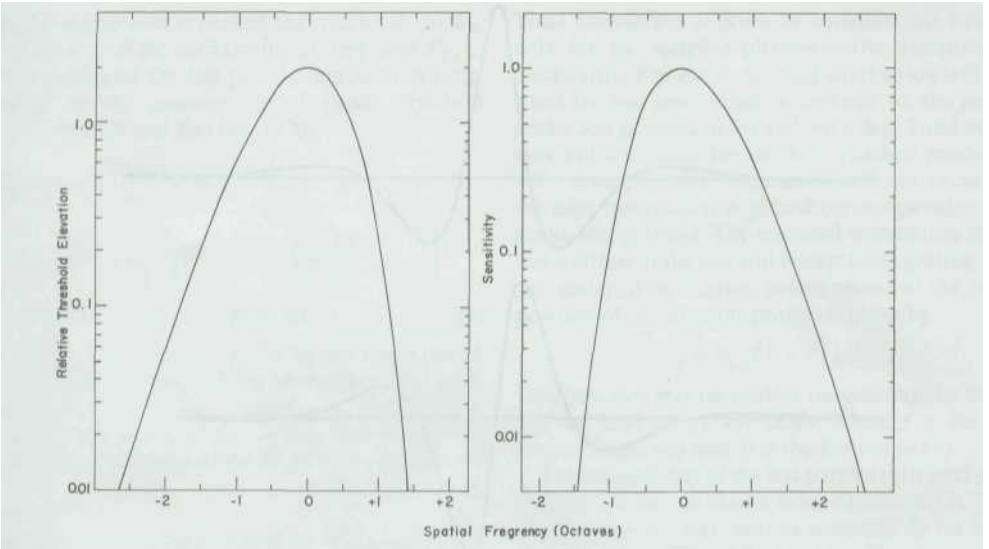

Fig. 7. On the left is the function that describes the relative threshold elevation produced by prolonged adaptation to gratings (Blakemore and Campbell, 1969). The spatial frequency of the adaptation grating is indicated by zero octaves on the abscissa—where the curve peaks. The abscissa shows the spatial frequency of the test grating relative to the adaptation spatial frequency. The ordinate indicates the log percentage elevation of the contrast threshold for detecting a grating after adaptation compared to before adaptation (e.g. the value 1·0 is equivalent to a 100 per cent threshold elevation). The curve on the right represents the hypothetical sensitivity function of each channel underlying these adaptation phenomena. It is assumed that the adaptation function directly reflects the sensitivity of the underlying mechanisms. Note that the sensitivity curve is a left–right inversion of the adaptation function (explained in Discussion). The ordinate shows log sensitivity, with the height of the peak normalized to 1·0. The abscissa represents the frequency on an octave scale relative to the peak channel frequency, which is designated zero octaves.

the form of the adaptation curve. The uninverted curve shows how one adapting frequency affects different test frequencies (different channels), whereas the inverted curve shows how one test frequency (one channel) is affected by different adapting frequencies. The asymmetry of the inverted curve shows that gratings that are higher than the peak frequency of the channel produce stronger adaptation of the channel than do gratings that are lower than the peak frequency the decline al *low* frequencies is thus sharper. This asymmetry is also observed in other studies on adaptation (Stecher, Sigel and Lange. 1973; Maudarbocus and Ruddock, 1973; Tolhurst. 1973) and masking (Stromeyer and Julesz, 1972).

An assumption is now made that this inverted curve reflects the *sensitivity* of the channels underlying these adaptation phenomena. The sensitivity curve is plotted intherighthalfofFig.7.ThesensitivityfunctionoftheJthchannelfortestgratingisgivenby f_T

$$\Phi(f_J/f_T) = \left[\frac{e^{-k(f_J/f_T)^2} - e^{-4k(f_J/f_T)^2}}{e^{-k} - e^{-4k}}\right]^2 \qquad (1)$$

where k = 0·462 is chosen so that the function peaks al f_T.= f_J . The height of the function is normalized to one. This expression is from Blakemore and Campbell.

A given sensitivity curve may arise from a variety of receptive field types. Figure 8 shows just two possible receptive fields (line spread functions) obtained by taking the Fourier transform of equation 1 with respect to f_T. [These receptive fields were originally presented in Stromeyer, Lange and Ganz (1973).] The general form of the equation of the receptive field, *RF*, as a function of x is given by

$$RF(x) = \int_0^\infty \Phi(f_J/f_T)\,(a\cos 2\pi f_T x + b\sin 2\pi f_T x]\,df_T. \qquad (2)$$

Maximal stimulation occurs for a sinusoidal grating whose half wavelength (horizontal peak to trough distance) matches the horizontal peak to trough distance of the receptive held.

The two mechanisms in Fig. 8 differ in sensitivity to the phase (position) of gratings relative to the center of the receptive field. The symmetric mechanism on the top is not sensitive to edge direction it will be called a bar mechanism. The antisymmetric mechanism on the bottom is maximally sensitive to an edge that is light on the left and dark on the right hence, an edge mechanism. In the present study, the 3·0 and 9·0 c/deg gratings were summed in peaks-add (triangle-wave) phase and peaks-subtract (square-wave) phase. The

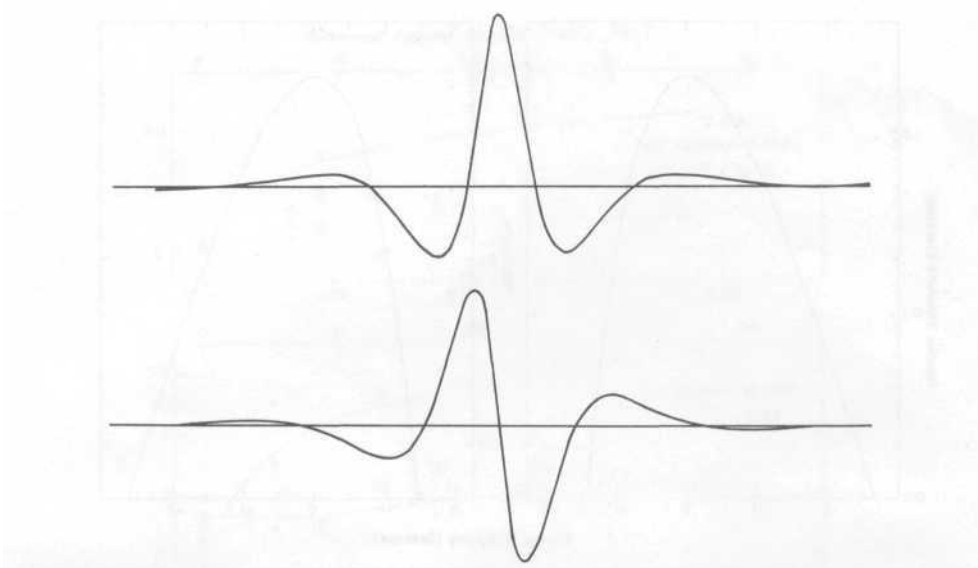

Fig. 8. Two possible receptive fields (line spread functions) obtained by taking the Fourier transform of the sensitivity function shown in Fig. 7. The symmetric mechanism is not sensitive to edge direction, and here it will be called a bar mechanism. The antisymmetric mechanism is more sensitive to an edge that is light on the left and dark on the right—an edge mechanism.

symmetric mechanism is maximally stimulated by the peaks-add gratings when the mechanism is centered on the peaks and is stimulated less for any position along the peaks-subtract gratings. Conversely, the antisymmetric mechanism is maximally stimulated by the peaks-subtract gratings when the mechanism is centered on the appropriate edge of the gratings (at the zero crossing). In the following model both the bar and edge mechanisms are examined. For convenience of notation, the phase-selective mechanism which is stimulated maximally by a given pattern of two gratings will be called the *matched* phase-selective mechanism, because its receptive field shape gives the better match to the stimulus profile. For example, the bar mechanism is matched to the peaks-add gratings. The other mechanism will thus be called the nonmatched phase-selective mechanism. (A comparison of the receptive fields in Fig. 8 and the stimuli profiles in Fig. 1 may help illustrate these points.)

The model predicts the expected detectability d' of the test grating as a function of the contrast, spatial frequency, and phase of the test and background gratings. The calculations include the following steps. First an expression is formulated which relates d to the contrast of the test grating presented alone. This relationship is called the transducer function. The data shows that d is an accelerated function of contrast. The acceleration is important for the task of discriminating the test plus background grating from the background grating by itself. The background grating may facilitate detection of the test grating by bringing the detection mechanism to a point where the transducer function is steeper. A weak test grating thus becomes more visible. The next equations describe how the *effective* contrast of two gratings (test and background) add within each channel. The transducer function can then be used to calculate how each channel discriminates the test pattern from the background—on the assumption that the optimal channel is used in the detection task.

In order to predict the detectability of the test gratings, an expression is needed for the transducer function which relates d' and grating contrast. Figure 2 shows detectability of the 9·0 c/deg test grating on a blank background as a function of contrast, for subject SK. The transducer function represented by the solid line is given by

$$d' = 5\bar{c}_T{}^4/(3 + 2\bar{c}_T{}^2) \tag{3}$$

where $\bar{c}_T$ is the contrast of the test pattern in units of "threshold" contrast. The threshold is *defined* as the contrast at which $d = 1$. The transducer function given by equation (3) will be used for all data. This transducer function has an acceleration (second derivative) which is approximately constant for $\bar{c}_T > 2$ and which falls quadratically to zero as $\bar{c}_T$ approaches zero. Transducer functions of the accelerated form $d \sim \bar{c}_T^p$, with an exponent p = 2-3, have been found for the detection of spots of light on a background (Nachmias and Kocher, 1970; Leshowitz, Taub and Raab, 1968) and for gratings (Nachmias and Sansbury, 1974; Klein *et al.*, in preparation). The transducer used for the present study has $p = 4$ for low $\bar{c}_T$ and $p = 2$ for large $\bar{c}_T$.

In order to predict the detectability of the test grating, denoted d_T, in the presence of the background

grating, an expression is needed that relates d_T to d'_B, the detectability of the background grating, and d'_{T+B}, the detectability of the test plus background grating. According to the assumptions of signal detection theory (Nachmias and Kocher, 1970)

$$\hat{d}_T = z_{T+B}\frac{\sigma_{T+B}}{\sigma_B} - z_B = \frac{\sigma_N}{\sigma_B}\left[z_{T+B}\frac{\sigma_{T+B}}{\sigma_N} - z_N - \left(z_B\frac{\sigma_B}{\sigma_N} - z_N\right)\right] = (d'_{T+B} - d'_B)/(1 + 0{\cdot}25\,d'_B) \quad (4)$$

where z_{T+B}, Z_B, Z_N are the z scores for yes responses to the test plus background grating, the background grating and the blank field. The quantities σ_{T+B}, σ_B, σ_N are the standard deviations of the various distributions. It is assumed that the slope of the ROC curve is given by $\sigma_N/\sigma_s = (1 + 0{\cdot}25\ d'_B)^{-1}$ (see also Nachmias and Kocher, 1970).

A prediction from these equations is shown by the solid line in Fig. 3. Figure 3 shows facilitation of the 9·0 c/deg test grating when added in phase on a 9·0 c/deg background grating. The contrast of the test grating is 0·82 times threshold contrast (test contrast, $\bar{c}_T$ 0·82 from Fig. 2). Maximal facilitation occurs for near-threshold background contrast; for higher background contrast, facilitation is reduced, as expected from Weber's law. For high background contrast equation (4) can be simplified to Weber's law

$$\hat{d}_T = \frac{p}{\alpha}\frac{\bar{c}_T}{\bar{c}_B}$$

where p is the exponent of the transducer function and a is related to the slope of the ROC curve by $\sigma_s/\sigma_N = 1 + \alpha d'$. The reduction in effective $\bar{c}_B$ due to adaptation is neglected. The values $p = 2$, a — 1/4 used in the present paper provide an adequate fit for high background contrasts.

Facilitation was also observed when the spatial frequency of the background grating was different from the test frequency. To predict the detectability of the test grating in this case, it is necessary to know the response of channels whose peak frequency lies between the test and background frequencies. The stimulation of channel J by test pattern T, that is, the *effective contrast* $\bar{c}_{J,T}$ of pattern T for channel J is given by

$$\bar{c}_{J,T} = \bar{c}_T \Phi(f_J/f_T) \quad (5)$$

where $\bar{c}_T$ is the contrast of the test grating in units of threshold contrast (i.e. the threshold for the whole visual system). Recall that Φ is normalized to one for $f_T = f_J$ [equation (1)]. This expression says that the effective contrast for channel J is simply the contrast (in units of threshold contrast) weighted by the channel sensitivity function. The *maximal* effective contrast for channel J produced by a test grating on a background grating is given by the sum of the effective contrasts of the test grating T and background grating B

$$\bar{c}_{J,T+B} = \bar{c}_T \Phi(f_J/f_T) + \bar{c}_B \Phi(f_J/f_T). \quad (6a)$$

Total summation as given by equation (6a) will occur only for the *matched* phase-selective receptive field mechanism. For example, total summation will occur when the bar mechanism is centered on the peaks of peaks-add gratings of 3·0 and 9·0 c/deg. Total summation will not occur for the non-matched mechanism—for example, total summation will *not* occur when the edge mechanism is placed on *any* position of the peaks-add gratings. The maximal summation of effective contrast of the test and background grating for the non-matched mechanism (when placed at the optimal position of the stimulus profile) is given by

$$\bar{c}_{J,T+B} = \bar{c}_{J,T}[1 + \bar{c}_{J,B}/3\bar{c}_{J,T}]^{3/2}. \quad (6b)$$

This equation was derived by maximizing the function $\bar{c}_{J,T}$ sin $2\pi fx + \bar{c}_{J,T}$ sin $2\pi 3fx$, where f is the background frequency and $3f$ is the test frequency.

The detectability of the test pattern on a background grating can be calculated from equations (3), (4) and (6). A computer was used to calculate $\hat{d}_T$ for a range of channels at different frequencies. The channel which yielded the highest value of $\hat{d}_T$ is defined to be the optimal channel. The peak frequency of the optimal channel lies between the background and test frequencies and varies with the contrast of the gratings. Table 1, for example, shows the peak frequency of the optimal channel for the matched phase-selective mechanism for different contrasts of the 3·0 c/deg background and 9·0 c/deg test gratings.

Table 1. Optimal channel for several $\bar{c}_B$, $\bar{c}_T$

$\bar{c}_B$	$\bar{c}_T$ 0·55	0·82	1·1
2	4·47 c/deg	4·54 c/deg	4·61 c/deg
4	5·12	5·18	5·26
8	5·71	5·78	5·83
16	6·26	6·32	6·38
32	6·77	6·82	6·88
64	7·24	7·29	7·34

The results of these calculations are shown by the curves in Figs. 4-6. The curves show the $\hat{d}_T$ value for the optimal channel. For these calculations, the threshold contrast value of the background gratings of 1·8 and 3·0 c/deg (where $\bar{c}_B = 1{\cdot}0$) was chosen to be one-half the threshold contrast value of the 9·0 c/deg test grating, because the photopic contrast sensitivity function shows that the threshold contrast for gratings of 1·8 and 3·0 c/deg is approximately one-half the value of the 9·0 c/deg grating (Campbell and Robson, 1968). For subject CFS the threshold contrast of the test grating on the blank background was chosen to be 25 per cent higher than the value for subject SK shown in Fig. 2, because measurements revealed that the difference in threshold for the two subjects was approximately this amount.

Figures 4 and 5 show detectability of the 9·0 c/deg test grating on the 3·0 c/deg background grating when the gratings are added in peaks-add phase (symbols in dotted cages) and peaks-subtract phases (symbols not in dotted cages). The solid line is the prediction for the matched phase-selective mechanism; the dashed line, the prediction for the non-matched phase-selective mechanism. Recall that the matched phase-selective mechanism is defined as that mechanism, symmetric or antisymmetric, which can totally summate the effective contrasts of the two gratings; the non-matched mechanism cannot totally summate the contrasts.

The edge mechanism is matched to the peaks-subtract gratings and non-matched to the peaks-add gratings. Conversely, the bar mechanism is matched to the peaks-add gratings and non-matched to the peaks-subtract gratings. The edge mechanism alone predicts most of the results. The edge mechanism is matched to the peaks-subtract grating, and is represented by the solid line—the line falls near the peaks-subtract data (not in dotted cages). The edge mechanism is non-matched to the peaks-add gratings, and is represented by the dashed line—the line falls only slightly below the peaks-add data (in dotted cages). The prediction of the non-matched bar mechanism—also represented by the dashed line—is far below the peaks-subtract data. Thus, the edge mechanism provides by far the better fit to the data.

In general it is seen that the theoretical calculation $\hat{d}_T$ is slightly higher than the data points. This discrepancy may have several explanations. (1) The form chosen for the transducer function and the channel sensitivity function may be slightly off. (2) Total linear summation of effective contrast of the test and background gratings may not occur since the actual edge mechanism may be typically asymmetric, not totally antisymmetric. Also, even though the visible background should allow attention to be focused upon the mechanism in the optimal position, in practice there will be contributions to d from non-optimal positions, thus decreasing the effective d'. (3) It has been found by Nachmias and Kocher that d'_T in a discrimination task is slightly less than $\hat{d}_T$ predicted by equation (4).

Figure 6 shows the predictions of the edge and bar mechanisms for detection of the test grating on the 1·8 c/deg background grating. The edge and bar mechanism are both matched phase-selective mechanism for this condition. Little facilitation is predicted, and no obvious facilitation was observed.

The results thus suggest that edge mechanisms are especially sensitive, and they may be used to detect gratings at threshold. The results in no way suggest that there are no symmetric bar mechanisms. The symmetric mechanisms may be simply less sensitive, or they may be tuned to a narrower range of spatial frequencies (and hence not influenced by the 3·0 c/deg background grating). The question of how to isolate such narrow-band mechanisms is not simple, because sensitive edge mechanisms would operate simultaneously in a detection task. The spatial frequency response of the edge mechanisms appears to be of medium bandwidth. The exact shape of a channel is not critical for our results. The only requirement is that the bandwidth be approximately the same as found in adaptation and masking studies. Evidence for yet narrower channels is provided by only one type of study (Sachs *et al,* 1971) and that study does not provide strong evidence for narrow-band channels (see Introduction).

The existence of edge mechanisms is further demonstrated by studies on single cortical cells of the cat (Bishop, Coombs and Henry, 1971) and monkey (Hubel and Wiesel, 1968). The hypothetical receptive fields in Fig. 8, calculated from the Blakemore and Campbell function, have extra excitatory and inhibitory zones which sharpen the frequency-selectivity of the mechanism. Such extra zones have been demonstrated in the cat at the level of retinal ganglion cells (Ikeda and Wright, 1972), LGN (Hammond, 1972, 1973; Maffei and Fiorentini, 1972) and cortex (Bishop, Henry and Smith, 1971).

Psychophysical adaptation studies (Gibson, 1933; Tolhurst, 1972; Stromeyer, Lange and Ganz, 1973) also suggest the existence of edge mechanisms. Shapley and Tolhurst (1973) and Kulkowski and King-Smith (1973) have attempted to measure the sensitivity profile of human edge detectors by observing how a subthreshold line affected the visibility of a subthreshold edge when the line was placed at various positions parallel to the edge. They explain their basic findings in terms of a class of edge detectors whose receptive field is of a single shape and size—in fact, a size optimally tuned to the peak of the sine-wave contrast sensitivity function (3-5 c/deg)—and whose frequency response is very broad. However, their results could also be explained by a *collection* of more narrowly tuned mechanisms. For example, for each position of the line relative to the edge, a different mechanism of slightly different receptive field size may be optimally excited, because the line and edge have a *very broad range* of spatial frequencies. The resultant sensitivity profile might thus represent the envelope of sensitivities of many more narrowly tuned mechanisms. Our results suggest that there are edge mechanisms with a range of sizes and which have a medium bandwidth frequency response.

Acknowledgements—We thank Professors Karl Pribram and Leo Ganz for their generous support and Dr. Arthur Lange for technical assistance and Mrs. Cecilia Bahlman for help with the manuscript.

REFERENCES

Bishop P. O., Coombs J. S. and Henry G. H. (1971) Interaction effects of visual contours on the discharge frequency of simple striate neurones. *J. Physiol, Lond.* **219,** 659-687.

Bishop P. O., Henry G. H. and Smith C. J. (1971) Binocular interaction fields of single units in the cat striate cortex. *J. Physiol., Lond.* 216, 39-68.

Blakemore C. and Campbell F. W. (1969) On the existence of neurones in the human visual system selectively sensi-

tive to the orientation and size of retinal images. *J. Physiol., Lond.* 203, 237-260.
Blakemore C. and Sutton P. (1969) Size adaptation; A new aftereffect. *Science, N.Y.* 166, 245-247.
Campbell F. W. and Green D. G. (1965) Optical and retinal factors affecting visual resolution. *J. Physiol., Lond.* 181, 576-593.
Campbell F. W. and Kulikowski J. J. (1966) Orientational selectivity of the human visual system. *J. Physiol., Lond.* 187, 437-445.
Campbell F. W. and Robson J. G. (1968) Application of Fourier analysis to the visibility of gratings. *J. Physiol., Lond.* 197, 551-566.
Egan J. P., Schulman A. I. and Greenberg G. Z. (1959) Operating characteristics determined by binary decisions and by ratings. *J. acoust. Soc. Am.* 31, 768-773.
Gibson J. J. (1933) Adaptation, after-effect and contrast in the perception of curved lines. *J. exp. Psychol.* 16, 1-31.
Graham N. (1972) Spatial frequency channels in the human visual system: Effects of luminance and pattern drift rate. *Vision Res.* 12, 53-68.
Hammond P. (1972) Spatial organization of receptive fields of LGN neurones. *J. Physiol., Lond.* 222, 53-54P.
Hammond P. (1973) Contrasts in spatial organization of receptive fields at geniculate and retinal levels: Centre, surround and outer surround. *J. Physiol., Lond.* 228, 115-137.
Hubel D. H. and Wiesel T. N. (1968) Receptive fields and functional architecture of monkey striate cortex. *J. Physiol., Lond.* 195,215-243.
Ikeda H. and Wright M. J. (1972) The outer disinhibitory surround of the retinal ganglion cell receptive field. *J. Physiol., Lond.* 226, 511-544.
Klein S., Stromeyer C. F. III and Ganz L. (1974) The simultaneous spatial frequency shift: A dissociation between the detection and perception of gratings. *Vision Res.* 14, 1421-1432.
Kulikowski J. J. and King-Smith P. E. (1973) Spatial arrangement of line, edge and grating detectors revealed by subthreshold summation. *Vision Res.* 13, 1455-1478.
Lange R. V., Sigel C. and Stecher S. (1973) Adapted and unadapted spatial frequency channels in human vision. *Vision Res. 13,* 2139-2144.'
Leshowitz B., Taub H. B. and Raab D. H. (1968) Visual detection of signals in the presence of continuous and pulsed backgrounds. *Percept. Psychophys.* 4, 207-213.
Maffei L. and Fiorentini A. (1972) Retinogeniculate convergence and analysis of contrast. *J. Neurophysiol.* 35, 65-72.
Maudarbocus A. Y. and Ruddock K. H. (1973) Non-linearity of visual signals in relation to shape-sensitive adaptation responses. *Vision Res.* 13, 1713-1737.
Nachmias J. and Kocher E. C. (1970) Visual detection and discrimination of luminance increments. *J. opt. Soc. Am.* **60,** 382-389.
Nachmias J. and Sansbury R. V. (1974) Grating contrast: Discrimination may be better than detection. *Vision Res.* **14,** 1039-1042.
Pantle A. and Sekuler R. (1968) Size-detecting mechanisms in human vision. *Science, N.Y.* 162, 1146-1148.
Sachs M. B., Nachmias J. and Robson J. G. (1971) Spatial-frequency channels in human vision. *J. opt. Soc. Am.* 61, 1176-1186.
Shapley R. M. and Tolhurst D. J. (1973) Edge detectors in human vision. *J. Physiol., Lond.* 229, 165-183.
Stecher S., Sigel C. and Lange R. V. (1973) Spatial frequency channels in human vision and the threshold for adaptation. *Vision Res.* 13, 1691-1700.
Stromeyer C. F. III and Julesz B. (1972) Spatial-frequency masking in vision: Critical bands and spread of masking. *J. opt. Soc. Am.* 62, 1221 1232.
Stromeyer C. F. III and Klein S. (1975) The detectability of frequency modulated gratings: Evidence against narrow-band spatial frequency channels in human vision. *Vision Res.* (in press).
Stromeyer C. F. III, Lange A. F. and Ganz L. (1973) Spatial frequency phase effects in human vision. *Vision Res.* 13, 2345-2360.
Tolhurst D. J. (1972) On the possible existence of edge detector neurones in the human visual system. *Vision Res.* 12,797-804.
Tolhurst D. J. (1973) Separate channels for the analysis of the shape and the movement of a moving visual stimulus. *J. Physiol., Lond.* 231, 385-402.

Resume—On mesure la possibilité de détecter un reseau sinusoidal de 9,0 c/deg en presence de fonds divers: champ uniforme, et reseaux de 3,0 c/deg ou 1,8 c/deg. La detection du reseau de 9,0 c/deg est facilitée par des fonds supraliminaux de reseaux a 3,0 c/deg (3,0 et 9,0 c/deg sont le premier et le troisième harmoniques), mais n'est pas facilitée par des fonds de reseaux a 1,8 c/deg (premier et cinquième harmoniques). On peut expliquer ces resultats par des canaux dont la sensibilite aux frequences spatiales ont une largeur de bande de une octave. Ces canaux repondent a la fois a des reseaux separes dans le rapport 1:3, mais ne repondent plus d'une facon significative au rapport 1:5. Ces resultats suggèrent que les canaux qui servent a la *detection des reseaux* ont une largeur de bande analogue aux canaux mis en evidence par les etudes d'adaptation et de masquage. L'analyse de la sensibilite a la phase suggere que ces mecanismes ont un champ recepteur asymétrique (mecanismes de bord).

Zusammenfassung—Die Erkennbarkeit eines Sinusgitters mit 9 Perioden/Grad wurde auf verschiedenem Untergrund gemessen. Ein leeres Feld, ein 3 Perioden/Grad-Gitter und ein 1,8 Perioden/Grad-Gitter. Die Erkennbarkeit des 9 Perioden/Grad-Gitters wurde durch ein überschwelliges Untergrundgitter von 3 Perioden/Grad verbessert (3 und 9 Perioden/Grad sind die 1 und 3 Harmonische), nicht jedoch durch das 1,8 Perioden/Grad-Gitter. Die Ergebnisse lassen sich durch Frequenzkanäle mit einer Bandbreite von einer Oktave erklären. Die Kanale antworten auf beide Gitter bei einem Frequenzverhältnis von 1:3, jedoch nicht, wenn beide Gitter durch ein Verhältnis von 1:5 getrennt sind. Die Ergebnisse lassen vermuten, dass die Kanale fur die *Erkennbarkeit von Gittern* eine ähnliche Bandbreite haben wie fur Gitteradaptation und Masking. Eine Analyse der Phasenempfindlichkeit weist darauf hin, dass die Mechanismen ein asymmetrisches rezeptives Feld haben.